Search for excited electrons in *ep* collisions at HERA

H1 Collaboration

F.D. Aaron [e,1], C. Alexa [e], V. Andreev [y], B. Antunovic [k], S. Aplin [k], A. Asmone [ag], A. Astvatsatourov [d], A. Bacchetta [k],
S. Backovic [ad], A. Baghdasaryan [al], P. Baranov [y,✠], E. Barrelet [ac], W. Bartel [k], M. Beckingham [k], K. Begzsuren [ai],
O. Behnke [n], A. Belousov [y], N. Berger [an], J.C. Bizot [aa], M.-O. Boenig [h], V. Boudry [ab], I. Bozovic-Jelisavcic [b], J. Bracinik [c],
G. Brandt [k], M. Brinkmann [k], V. Brisson [aa], D. Bruncko [p], A. Bunyatyan [m,al], G. Buschhorn [z], L. Bystritskaya [x],
A.J. Campbell [k], K.B. Cantun Avila [v], F. Cassol-Brunner [u], K. Cerny [af], V. Cerny [p,2], V. Chekelian [z], A. Cholewa [k],
J.G. Contreras [v], J.A. Coughlan [f], G. Cozzika [j], J. Cvach [ae], J.B. Dainton [r], K. Daum [ak,3], M. Deák [k], Y. de Boer [k],
B. Delcourt [aa], M. Del Degan [an], J. Delvax [d], A. De Roeck [k,4], E.A. De Wolf [d], C. Diaconu [u,*], V. Dodonov [m],
A. Dossanov [z], A. Dubak [ad,5], G. Eckerlin [k], V. Efremenko [x], S. Egli [aj], A. Eliseev [y], E. Elsen [k], S. Essenov [x],
A. Falkiewicz [g], P.J.W. Faulkner [c], L. Favart [d], A. Fedotov [x], R. Felst [k], J. Feltesse [j,6], J. Ferencei [p], L. Finke [k],
M. Fleischer [k], A. Fomenko [y], E. Gabathuler [r], J. Gayler [k], S. Ghazaryan [al], A. Glazov [k], I. Glushkov [am], L. Goerlich [g],
M. Goettlich [l], N. Gogitidze [y], M. Gouzevitch [ab], C. Grab [an], T. Greenshaw [r], B.R. Grell [k], G. Grindhammer [z], S. Habib [l,7],
D. Haidt [k], M. Hansson [t], C. Helebrant [k], R.C.W. Henderson [q], H. Henschel [am], G. Herrera [w], M. Hildebrandt [aj],
K.H. Hiller [am], D. Hoffmann [u], R. Horisberger [aj], A. Hovhannisyan [al], T. Hreus [d,8], M. Jacquet [aa], M.E. Janssen [k],
X. Janssen [d], V. Jemanov [l], L. Jönsson [t], D.P. Johnson [d,✠], A.W. Jung [o], H. Jung [k], M. Kapichine [i], J. Katzy [k], I.R. Kenyon [c],
C. Kiesling [z], M. Klein [r], C. Kleinwort [k], T. Klimkovich, T. Kluge [r], A. Knutsson [k], R. Kogler [z], V. Korbel [k], P. Kostka [am],
M. Kraemer [k], K. Krastev [k], J. Kretzschmar [r], A. Kropivnitskaya [x], K. Krüger [o], K. Kutak [k], M.P.J. Landon [s], W. Lange [am],
G. Laštovička-Medin [ad], P. Laycock [r], A. Lebedev [y], G. Leibenguth [an], V. Lendermann [o], S. Levonian [k], G. Li [aa], K. Lipka [l],
A. Liptaj [z], B. List [l], J. List [k], N. Loktionova [y], R. Lopez-Fernandez [w], V. Lubimov [x], A.-I. Lucaci-Timoce [k], L. Lytkin [m],
A. Makankine [i], E. Malinovski [y], P. Marage [d], Ll. Marti [k], H.-U. Martyn [a], S.J. Maxfield [r], A. Mehta [r], K. Meier [o],
A.B. Meyer [k], H. Meyer [k], H. Meyer [ak], J. Meyer [k], V. Michels [k], S. Mikocki [g], I. Milcewicz-Mika [g], F. Moreau [ab],
A. Morozov [i], J.V. Morris [f], M.U. Mozer [d], M. Mudrinic [b], K. Müller [ao], P. Murín [p,8], K. Nankov [ah], B. Naroska [l,✠],
Th. Naumann [am], P.R. Newman [c], C. Niebuhr [k], A. Nikiforov [k], G. Nowak [g], K. Nowak [ao], M. Nozicka [k], B. Olivier [z],
J.E. Olsson [k], S. Osman [t], D. Ozerov [x], V. Palichik [i], I. Panagoulias [k,9,10], M. Pandurovic [b], Th. Papadopoulou [k,9,10],
C. Pascaud [aa], G.D. Patel [r], O. Pejchal [af], H. Peng [k], E. Perez [j,4], A. Petrukhin [x], I. Picuric [ad], S. Piec [am], D. Pitzl [k],
R. Plačakytė [k], R. Polifka [af], B. Povh [m], T. Preda [e], V. Radescu [k], A.J. Rahmat [r], N. Raicevic [ad], A. Raspiareza [z],
T. Ravdandorj [ai], P. Reimer [ae], E. Rizvi [s], P. Robmann [ao], B. Roland [d], R. Roosen [d], A. Rostovtsev [x], M. Rotaru [e],
J.E. Ruiz Tabasco [v], Z. Rurikova [k], S. Rusakov [y], D. Salek [af], F. Salvaire [k], D.P.C. Sankey [f], M. Sauter [an], E. Sauvan [u],
S. Schmidt [k], S. Schmitt [k], C. Schmitz [ao], L. Schoeffel [j], A. Schöning [k,ao], H.-C. Schultz-Coulon [o], F. Sefkow [k],
R.N. Shaw-West [c], I. Sheviakov [y], L.N. Shtarkov [y], S. Shushkevich [z], T. Sloan [q], I. Smiljanic [b], P. Smirnov [y], Y. Soloviev [y],
P. Sopicki [g], D. South [h], V. Spaskov [i], A. Specka [ab], Z. Staykova [k], M. Steder [k], B. Stella [ag], U. Straumann [ao], D. Sunar [d],
T. Sykora [d], V. Tchoulakov [i], G. Thompson [s], P.D. Thompson [c], T. Toll [k], F. Tomasz [p], T.H. Tran [aa], D. Traynor [s],
T.N. Trinh [u], P. Truöl [ao], I. Tsakov [ah], B. Tseepeldorj [ai,11], I. Tsurin [am], J. Turnau [g], E. Tzamariudaki [z], K. Urban [o],
A. Valkárová [af], C. Vallée [u], P. Van Mechelen [d], A. Vargas Trevino [k], Y. Vazdik [y], S. Vinokurova [k], V. Volchinski [al],
D. Wegener [h], M. Wessels [k], Ch. Wissing [k], E. Wünsch [k], V. Yeganov [al], J. Žáček [af], J. Zálešák [ae], Z. Zhang [aa],
A. Zhelezov [x], A. Zhokin [x], Y.C. Zhu [k], T. Zimmermann [an], H. Zohrabyan [al], F. Zomer [aa]

[a] *I. Physikalisches Institut der RWTH, Aachen, Germany [12]*
[b] *Vinca Institute of Nuclear Sciences, Belgrade, Serbia*
[c] *School of Physics and Astronomy, University of Birmingham, Birmingham, UK [13]*
[d] *Inter-University Institute for High Energies ULB-VUB, Universiteit Antwerpen, Antwerpen, Belgium [14]*
[e] *National Institute for Physics and Nuclear Engineering (NIPNE), Bucharest, Romania*
[f] *Rutherford Appleton Laboratory, Chilton, Didcot, UK [13]*
[g] *Institute for Nuclear Physics, Cracow, Poland [15]*

[h] *Institut für Physik, TU Dortmund, Dortmund, Germany* [12]
[i] *Joint Institute for Nuclear Research, Dubna, Russia*
[j] *CEA, DSM/DAPNIA, CE-Saclay, Gif-sur-Yvette, France*
[k] *DESY, Hamburg, Germany*
[l] *Institut für Experimentalphysik, Universität Hamburg, Hamburg, Germany* [12]
[m] *Max-Planck-Institut für Kernphysik, Heidelberg, Germany*
[n] *Physikalisches Institut, Universität Heidelberg, Heidelberg, Germany* [12]
[o] *Kirchhoff-Institut für Physik, Universität Heidelberg, Heidelberg, Germany* [12]
[p] *Institute of Experimental Physics, Slovak Academy of Sciences, Košice, Slovak Republic* [16]
[q] *Department of Physics, University of Lancaster, Lancaster, UK* [13]
[r] *Department of Physics, University of Liverpool, Liverpool, UK* [13]
[s] *Queen Mary and Westfield College, London, UK* [13]
[t] *Physics Department, University of Lund, Lund, Sweden* [17]
[u] *CPPM, CNRS/IN2P3, Univ. Mediterranee, Marseille, France*
[v] *Departamento de Fisica Aplicada, CINVESTAV, Mérida, Yucatán, Mexico* [18]
[w] *Departamento de Fisica, CINVESTAV, Mexico* [18]
[x] *Institute for Theoretical and Experimental Physics, Moscow, Russia*
[y] *Lebedev Physical Institute, Moscow, Russia* [19]
[z] *Max-Planck-Institut für Physik, München, Germany*
[aa] *LAL, Université Paris-Sud, CNRS/IN2P3, Orsay, France*
[ab] *LLR, Ecole Polytechnique, IN2P3-CNRS, Palaiseau, France*
[ac] *LPNHE, Universités Paris VI and VII, IN2P3-CNRS, Paris, France*
[ad] *Faculty of Science, University of Montenegro, Podgorica, Montenegro* [19]
[ae] *Institute of Physics, Academy of Sciences of the Czech Republic, Praha, Czech Republic* [20]
[af] *Faculty of Mathematics and Physics, Charles University, Praha, Czech Republic* [20]
[ag] *Dipartimento di Fisica, Università di Roma Tre and INFN Roma 3, Roma, Italy*
[ah] *Institute for Nuclear Research and Nuclear Energy, Sofia, Bulgaria* [19]
[ai] *Institute of Physics and Technology of the Mongolian Academy of Sciences, Ulaanbaatar, Mongolia*
[aj] *Paul Scherrer Institut, Villigen, Switzerland*
[ak] *Fachbereich C, Universität Wuppertal, Wuppertal, Germany*
[al] *Yerevan Physics Institute, Yerevan, Armenia*
[am] *DESY, Zeuthen, Germany*
[an] *Institut für Teilchenphysik, ETH, Zürich, Switzerland* [21]
[ao] *Physik-Institut der Universität Zürich, Zürich, Switzerland* [21]

ARTICLE INFO

ABSTRACT

A search for excited electrons is performed using the full $e^{\pm}p$ data sample collected by the H1 experiment at HERA, corresponding to a total luminosity of 475 pb^{-1}. The electroweak decays of excited electrons $e^* \to e\gamma$, $e^* \to eZ$ and $e^* \to \nu W$ with subsequent hadronic or leptonic decays of the W and Z bosons are considered. No evidence for excited electron production is found. Mass dependent exclusion limits on e^* production cross sections and on the ratio f/Λ of the coupling to the compositeness scale are derived within gauge mediated models. These limits extend the excluded region compared to previous excited electron searches. The e^* production via contact interactions is also addressed for the first time in ep collisions.

© 2008 Elsevier B.V. All rights reserved.

* Corresponding author.
 E-mail address: diaconu@cppm.in2p3.fr (C. Diaconu).

1. Introduction

The three-family structure and mass hierarchy of the known fermions is one of the most puzzling characteristics of the Standard Model (SM) of particle physics. Attractive explanations are provided by models assuming composite quarks and leptons [1]. The existence of excited states of leptons and quarks is a natural consequence of these models and their discovery would provide convincing evidence of a new scale of matter. Electron[22]–proton interactions at very high energies provide good conditions to search for excited states of first generation fermions. For instance, excited electrons (e^*) could be singly produced through the exchange of a γ or a Z boson in the t-channel.

In this Letter a search for excited electrons using the complete $e^\pm p$ HERA collider data of the H1 experiment is presented. Electroweak decays into a SM lepton (e, ν_e) and a SM gauge boson (γ, W and Z) are considered and hadronic as well as leptonic decays of the W and Z are analysed.

The data are recorded at electron beam energy of 27.6 GeV and proton beam energies of 820 GeV and 920 GeV, corresponding to centre-of-mass energies $\sqrt{s}$ of 301 GeV and 319 GeV, respectively. The total integrated luminosity of the data is 475 pb^{-1}. The data comprise 184 pb^{-1} recorded in e^-p collisions and 291 pb^{-1} in e^+p collisions, of which 35 pb^{-1} were recorded at $\sqrt{s} = 301$ GeV. With a four-fold increase in statistics, this analysis supersedes the result of the previous H1 search for excited electrons [2]. It complements the search for excited neutrinos [3].

2. Excited electron models

In the present study a model [4–6] is considered in which excited fermions are assumed to have spin 1/2 and isospin 1/2. The left-handed and right-handed components of the excited fermions form weak iso-doublets F_L^* and F_R^*.

Interactions between excited and ordinary fermions may be mediated by gauge bosons, as described by the effective Lagrangian [5,6]:

$$\mathcal{L}_{\text{GM}} = \frac{1}{2\Lambda} \bar{F}_R^* \sigma^{\mu\nu} \left[gf \frac{\tau^a}{2} W_{\mu\nu}^a + g'f' \frac{Y}{2} B_{\mu\nu} + g_s f_s \frac{\lambda^a}{2} G_{\mu\nu}^a \right] F_L + \text{h.c.}$$
(1)

Only the right-handed component of the excited fermion F_R^* is allowed to couple to light fermions, in order to protect the light leptons from radiatively acquiring a large anomalous magnetic moment [7,8]. The matrix $\sigma^{\mu\nu}$ is the covariant bilinear tensor, $W_{\mu\nu}^a$, $B_{\mu\nu}$ and $G_{\mu\nu}^a$ are the field-strength tensors of the SU(2), U(1) and SU(3)$_C$ gauge fields, τ^a, Y and λ^a are the Pauli matrices, the weak hypercharge operator and the Gell-Mann matrices, respectively. The standard electroweak and strong gauge couplings are denoted by g, g' and g_s, respectively. The parameter Λ has units of energy and can be regarded as the compositeness scale which reflects the range of the new confinement force. The constants f, f' and f_s are coupling parameters associated to the three gauge groups and are determined by the yet unknown composite dynamics.

Following this model of gauge mediated (GM) interactions, single e^* production in ep collisions may result from the t-channel exchange of a γ or Z boson. Since the e^* is expected not to have strong interactions, the present search is insensitive to f_s. The produced e^* may decay into a lepton and an electroweak gauge boson via $e^* \to e\gamma$, $e^* \to \nu W$ and $e^* \to eZ$. For a given e^* mass value M_{e^*} and assuming a numerical relation between f and f', the e^* branching ratios are fixed and the production cross section depends only on f/Λ. In most analyses the assumption is made that the coupling parameters f and f' are of comparable strength and only the relationships $f = -f'$ and $f = +f'$ are considered. In the case $f = -f'$, the excited electron does not couple to the photon and therefore the e^* production cross section at HERA is small. Therefore, only the case $f = +f'$ is considered in this analysis.

In addition to GM interactions, novel composite dynamics may be visible as contact interactions (CI) between excited fermions and SM quarks and leptons. Such interactions can be described by the effective four-fermion Lagrangian [5]:

$$\mathcal{L}_{\text{CI}} = \frac{4\pi}{2\Lambda^2} j^\mu j_\mu,$$
(2)

where Λ is assumed to be the same parameter as in the Lagrangian (1) and j_μ is the fermion current

$$j_\mu = \eta_L \bar{F}_L^* \gamma_\mu F_L + \eta_L' \bar{F}_L \gamma_\mu F_L + \eta_L'' \bar{F}_L^* \gamma_\mu F_L^* + \text{h.c.} + (L \to R).$$
(3)

Conventionally, the η factors are set to one for the left-handed and to zero for the right-handed current.

Contact interactions may induce changes in the cross section of neutral current (NC) deep-inelastic scattering (DIS) $ep \to eX$. Searches for deviations from the SM cross section at the highest squared momentum transfers Q^2 in NC DIS processes have excluded values of Λ between 1.6 TeV and 5.5 TeV, depending on the chiral structure considered [9]. Contact interactions may also mediate the resonant production of excited electrons in ep collisions as well as their decays into an electron and a pair of SM fermions. The e^* production and decay by both gauge and contact interactions is also considered in this analysis. In this case the total e^* production cross section $\sigma_{\text{GM+CI}}$ is the sum of pure GM and CI cross sections and of the interference between the two processes [10]. For simplicity, the relative strength of gauge and contact interactions are fixed by setting the parameters f and f' of the gauge interaction to one. The ratio of the GM + CI and GM cross sections $\sigma_{\text{GM+CI}}/\sigma_{\text{GM}}$ then depends only on Λ and on the e^* mass. For $M_{e^*} = 150$ GeV and $\Lambda = 1$ TeV, $\sigma_{\text{GM+CI}}/\sigma_{\text{GM}}$ is equal to 8.4, but reduces to 1.3 for $\Lambda = 4$ TeV. Relative branching ratios of GM and CI decays are determined by the e^* partial widths in each decay channel [5]. In the sensitive domain of the present analysis ($\Lambda \simeq 4$ TeV and 100 GeV $< M_{e^*} < 200$ GeV), more than 95% of e^* decays are gauge mediated. Therefore, only GM decay channels are used for the present search.

3. Simulation of signal and background processes

The Monte Carlo (MC) event generator COMPOS [11] is used for the calculation of the e^* production cross section and to determine the signal detection efficiencies. It is based on the cross section formulae for gauge mediated interactions [4,5]. Cross section formulae for contact interaction production and for the interference between contact and gauge interactions [10] have also been incorporated into COMPOS. Only e^* decays via gauge mediated interactions are simulated. Initial state radiation of a photon from the incident electron is included using the Weizsäcker–Williams approximation [12]. The proton parton densities are taken from the CTEQ5L [13] parametrisation and are evaluated at the scale $\sqrt{Q^2}$. The parton shower approach [14] is applied in order to simulate Quantum Chromodynamics (QCD) corrections in the initial and final states. Hadronisation is performed using Lund string fragmentation as implemented in PYTHIA [14]. The COMPOS generator uses the narrow width approximation (NWA) for the calculation of the production cross section and takes into account the natural width of the excited electron for the e^* decay. The NWA is valid for e^* masses below 290 GeV and the couplings f/Λ relevant to this analysis, as the total e^* width is less than 10% of the e^* mass.

The Standard Model (SM) processes which may mimic the e^* signal are QED Compton scattering, neutral current and charged current (CC) deep-inelastic scattering and to a lesser extent photoproduction, lepton pair production and real W boson production. All SM processes are generated with at least 10 times the integrated luminosity of the data sample.

The RAPGAP [15] event generator, which implements the Born, QCD Compton and Boson Gluon Fusion matrix elements, is used to model NC DIS events. The QED radiative effects arising from real photon emission from both the incoming and outgoing electrons are simulated using the HERACLES [16] program. Direct and resolved photoproduction of jets and prompt photon production are simulated using the PYTHIA event generator. The simulation is based on Born level hard scattering matrix elements with radiative QED corrections. In RAPGAP and PYTHIA, jet production from higher order QCD radiation is simulated using leading log-

arithmic parton showers and hadronisation is modelled with Lund string fragmentation. The leading order MC prediction of NC DIS and photoproduction processes with two or more high transverse momentum jets is scaled by a factor of 1.2 to account for missing higher order QCD contributions in the MC generators [19,20]. Charged current DIS events are simulated using the DJANGO [17] program, which includes first order leptonic QED radiative corrections based on HERACLES. The production of two or more jets in DJANGO is accounted for using the colour-dipole model [18]. Contributions from elastic and quasi-elastic QED Compton scattering are simulated with the WABGEN [21] generator. Contributions arising from the production of W bosons and multi-lepton events are modelled using the EPVEC [22] and GRAPE [23] event generators, respectively.

Generated events are passed through the full GEANT [24] based simulation of the H1 apparatus, which takes into account the actual running conditions of the data taking, and are reconstructed and analysed using the same program chain as for the data.

4. Experimental conditions

A detailed description of the H1 experiment can be found in [25]. Only the detector components relevant to the present analysis are briefly described here. The origin of the H1 coordinate system is the nominal ep interaction point, with the direction of the proton beam defining the positive z-axis (forward region). Transverse momentum (P_T) is measured in the xy plane. The pseudorapidity η is related to the polar angle θ by $\eta = -\ln \tan(\theta/2)$. The Liquid Argon (LAr) calorimeter [26] is used to measure electrons, photons and hadrons. It covers the polar angle range $4° < \theta < 154°$ with full azimuthal acceptance. Electromagnetic shower energies are measured with a precision of $\sigma(E)/E = 12\%/\sqrt{E/\text{GeV}} \oplus 1\%$ and hadronic energies with $\sigma(E)/E = 50\%/\sqrt{E/\text{GeV}} \oplus 2\%$, as measured in test beams [27,28]. In the backward region, energy measurements are provided by a lead/scintillating-fiber (SpaCal) calorimeter [29] covering the angular range $155° < \theta < 178°$. The central ($20° < \theta < 160°$) and forward ($7° < \theta < 25°$) tracking detectors are used to measure charged particle trajectories, to reconstruct the interaction vertex and to complement the measurement of hadronic energy. The LAr and inner tracking detectors are enclosed in a super-conducting magnetic coil with a field strength of 1.16 T. The return yoke of the coil is the outermost part of the detector and is equipped with streamer tubes forming the central muon detector ($4° < \theta < 171°$). In the forward region of the detector ($3° < \theta < 17°$) a set of drift chambers detects muons and measures their momenta using an iron toroidal magnet. The luminosity is determined from the rate of the Bethe–Heitler process $ep \rightarrow ep\gamma$, measured using a photon detector located close to the beam pipe at $z = -103$ m, in the backward direction.

5. Data analysis

The triggers employed for collecting the data used in this analysis are based on the detection of electromagnetic deposits or missing transverse energy in the LAr calorimeter [30]. The trigger efficiency is $\sim 90\%$ for events with missing transverse energy of 20 GeV, and increases above 95% for missing transverse energy above 30 GeV. Events containing an electromagnetic deposit (electron or photon) with an energy greater than 10 GeV are triggered with an efficiency close to 100%.

In order to remove background events induced by cosmic showers and other non-ep sources, the event vertex is required to be reconstructed within 35 cm in z of the nominal interaction point. In addition, topological filters and timing vetoes are applied.

The identification of electrons or photons relies on the measurement of a compact and isolated electromagnetic shower in

the LAr calorimeter. The hadronic energy within a distance in the pseudorapidity–azimuth (η-ϕ) plane $R = \sqrt{\Delta\eta^2 + \Delta\phi^2} < 0.5$ around the electron (photon) is required to be below 3% of the electron (photon) energy. Furthermore, each electron (photon) candidate must be isolated from jets by a minimum distance in pseudorapidity–azimuth of $R > 0.5$ to any jet axis. The electron and photon energy and angular direction are measured by the calorimeters. Muon identification is based on a track measured in the inner tracking systems associated with signals in the muon detectors [31]. A muon candidate is required to have no more than 5 GeV deposited in a cylinder, centred on the muon track direction, of radius 25 cm and 50 cm in the electromagnetic and hadronic sections of the LAr calorimeter, respectively. Additionally, the muon candidate is required to be separated from the closest jet and from any track by $R > 1$ and $R > 0.5$, respectively. Calorimeter energy deposits and tracks not previously identified as electron, photon or muon candidates are used to form combined cluster-track objects, from which the hadronic energy is reconstructed [32,33]. Jets are reconstructed from these combined cluster-track objects using an inclusive k_T algorithm [34,35] with a minimum transverse momentum of 2.5 GeV. The missing transverse momentum P_T^{miss} of the event is derived from all detected particles and energy deposits in the event. In events with large P_T^{miss}, the only non-detected particle in the event is assumed to be a neutrino. The four-vector of this neutrino candidate is reconstructed assuming transverse momentum conservation and the relation $\sum_i(E^i - P_z^i) + (E^\nu - P_z^\nu) = 2E_e^0 = 55.2$ GeV, where the sum runs over all detected particles, P_z is the momentum along the proton beam axis and E_e^0 is the electron beam energy.

Specific selection criteria applied in each decay channel are presented in the following subsections. A detailed description of the analysis can be found in [36].

5.1. $e\gamma$ resonance search

The signature of the $e^* \rightarrow e\gamma$ decay channel consists of two high P_T isolated electromagnetic clusters. SM background arises mainly from elastic and inelastic QED Compton events. Two isolated electromagnetic clusters are required, each with transverse momentum $P_T > 15$ GeV and polar angle $5° < \theta < 130°$. No explicit electron and photon identification based on tracking conditions is performed in order to retain a high selection efficiency. To reduce contributions from QED Compton processes, the sum of the energies of the two electromagnetic clusters is required to be greater than 110 GeV and the sum of their total transverse momenta has to be larger than 75 GeV.

After this selection, the SM background from elastic QED Compton events is smaller than that from inelastic QED Compton processes. Since about half of the e^* production cross section is expected from elastic e^* production [4], the analysis is separated into two parts. Events with a total hadronic energy $E_h < 5$ GeV are used to search for elastic e^* production, whereas the other events are attributed to possible inelastic e^* production.

In the elastic channel 42 events are selected in the data compared to a SM expectation of 48 ± 4. In the inelastic channel 65 events are found for 65 ± 8 expected. The errors on the SM prediction include model and experimental systematic errors added in quadrature (see Section 5.5). The invariant mass of the e^* candidate is calculated from the four-vectors of the electron and photon candidates. The invariant mass distribution of the e^* candidates and the SM background expectations are presented in Fig. 1(a) and (b) for the elastic and inelastic channels, respectively. The selection efficiency is 60% for $M_{e^*} = 120$ GeV, increasing to 70% for $M_{e^*} = 260$ GeV. From Monte Carlo studies, the experimental resolution on the reconstructed e^* mass distribution is 3 GeV for a
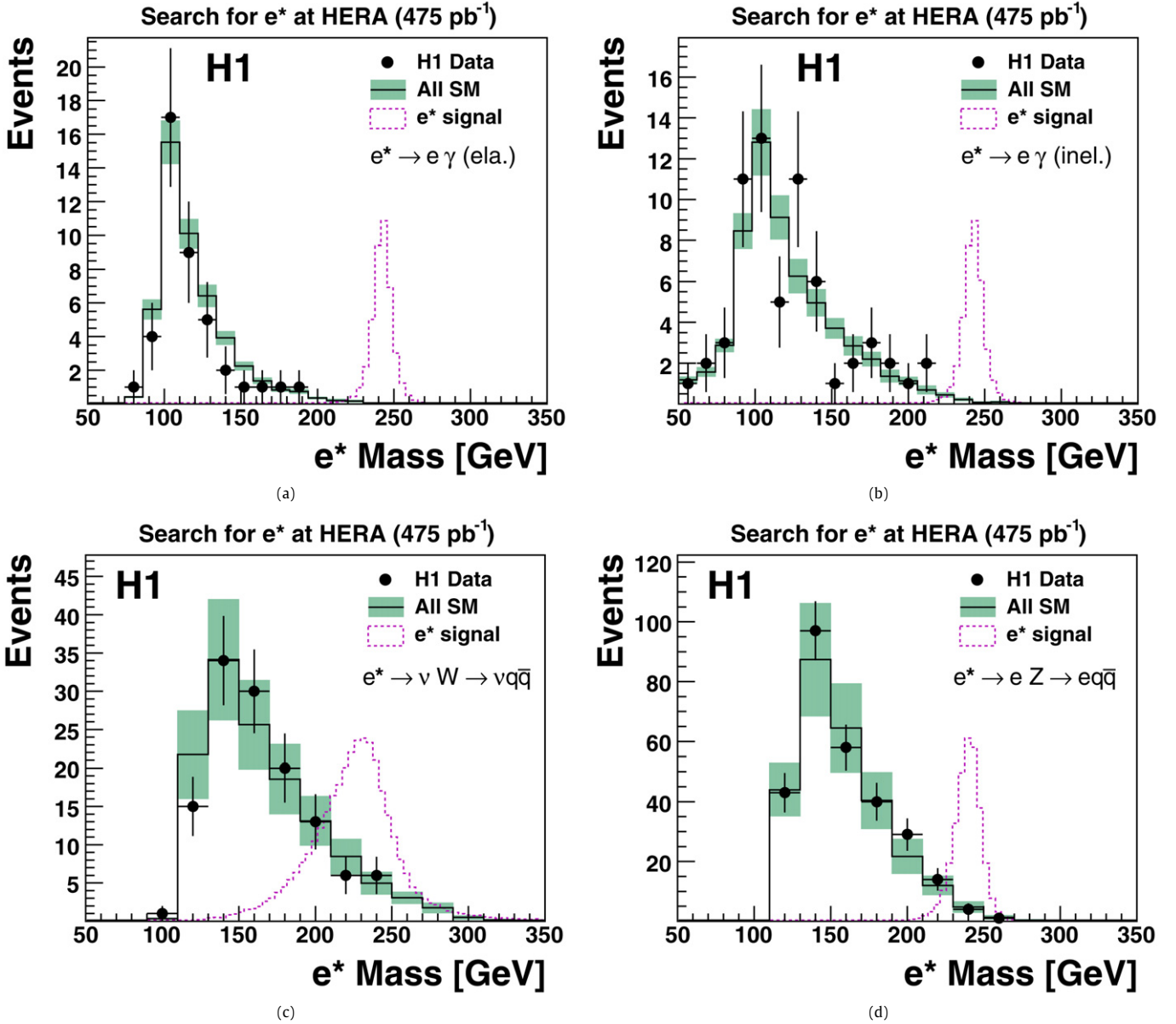
Fig. 1. Invariant mass distribution of the e^* candidates in the elastic $e^* \to e\gamma$ (a), inelastic $e^* \to e\gamma$ (b), $e^* \to \nu W \to \nu q\bar{q}$ (c), and $e^* \to eZ \to eq\bar{q}$ (d) search channels. The points correspond to the observed data events and the histograms to the SM expectation after the final selections. The error bands on the SM prediction include model uncertainties and experimental systematic errors added in quadrature. The dashed line represents with an arbitrary normalisation the reconstructed mass distribution of e^* events with $M_{e^*} = 240$ GeV.

generated e^* mass of 120 GeV, increasing to 6 GeV for an e^* mass of 260 GeV.

5.2. $\nu q\bar{q}$ resonance search

The signature of the $e^* \to \nu W \to \nu q\bar{q}$ decay channel consists of two high transverse momentum jets in events with large P_T^{miss}. The SM background is dominated by multi-jet CC DIS events and contains moderate contributions from NC DIS and photoproduction. Events with missing transverse momentum $P_T^{\text{miss}} > 20$ GeV are selected. In each event at least two jets with transverse momenta larger than 20 and 15 GeV, respectively, are required in the polar angle range $5° < \theta < 130°$.

The ratio V_{ap}/V_p of transverse energy flow anti-parallel and parallel to the hadronic final state [37] is used to suppress photoproduction events. Events with $V_{ap}/V_p > 0.3$ are rejected. Photoproduction and NC DIS backgrounds typically have low values of x_h, the Bjorken scaling variable calculated from the hadronic

system using the Jacquet–Blondel method [37,38], and are thus suppressed by requiring $x_h > 0.04$. In each event, a W candidate is reconstructed from the combination of those two jets with invariant mass closest to the nominal W boson mass. The reconstructed W candidate is required to have an invariant mass above 60 GeV. In order to further reduce the background from CC DIS, the invariant mass of all jets and hadrons in the event not associated to the decay of the W boson candidate is required to be below 15 GeV.

After this selection, 129 events are found compared to a SM expectation of 133 ± 32 events which is dominated by CC DIS events. The CC DIS cross section is smaller in e^+p collisions than in e^-p, in contrast to the e^* cross section which is comparable in both collision modes. Therefore, e^+p data have a larger sensitivity to a potential e^* signal in this channel than e^-p data. In the e^+p (e^-p) data sample, 33 (96) events are observed compared to a SM expectation of 51 ± 13 (82 ± 19). A significant excess is observed neither in e^+p nor in e^-p data. The invariant mass of the e^* candi-

date is calculated from the neutrino and W candidate four-vectors. For this calculation, the W candidate four-vector is scaled such that its mass is set to the nominal W boson mass. The invariant mass distributions of the e^* candidates and the SM background are presented in Fig. 1(c). The selection efficiency in this channel is 20% for $M_{e^*} = 120$ GeV, increasing to 55% for $M_{e^*} = 260$ GeV. From Monte Carlo studies, the experimental resolution on the reconstructed e^* mass distribution is 9 GeV for a generated e^* mass of 120 GeV, increasing to ~ 20 GeV for an e^* mass of 260 GeV.

5.3. *eqq̄ resonance search*

The signature of the $e^* \to eZ \to eq\bar{q}$ decay channel consists of one electron and two high P_T jets. Multi-jet NC DIS events constitute the main background contribution from SM processes. Events are selected with an isolated electron in the LAr calorimeter in the polar angle range $5° < \theta^e < 90°$. The electron should have either a transverse momentum P_T^e greater than 25 GeV or the variable[23] $\xi^e = E^e \cos^2(\theta^e/2)$ above 23 GeV. These conditions remove a large part of the NC DIS contribution. The events are required to have at least two jets in the polar angle range $5° < \theta^{jet} < 130°$ with transverse momenta larger than 20 and 15 GeV, respectively. In each event, a Z candidate is reconstructed from the combination of those two jets with invariant mass closest to the nominal Z boson mass. The reconstructed mass of the Z candidate is required to be larger than 70 GeV. To further reduce the NC DIS background the polar angle of the jet with the highest P_T associated to the Z candidate is required to be less than 80°. The polar angle of the second jet is required to be greater than 10° in events with $P_T^{jet_2} < 25$ GeV.

After this selection, 286 events are observed while 277 ± 62 are expected from the SM. The invariant mass of the e^* candidate is calculated from the electron and Z candidate four-vectors. For this calculation, the Z candidate four-vector is scaled such that its mass is set to the nominal Z boson mass. The invariant mass distributions of the e^* candidates and the SM background are presented in Fig. 1(d). The selection efficiency in this channel is 20% for $M_{e^*} = 120$ GeV, increasing to 55% for $M_{e^*} = 260$ GeV. From Monte Carlo studies, the experimental resolution on the reconstructed e^* mass distribution is 2 GeV for a generated e^* mass of 120 GeV, increasing to 8 GeV for an e^* mass of 260 GeV.

5.4. *eee, eμμ and eνν resonance searches*

In the search for $e^* \to eZ \to eee$, events with three electrons of high transverse momenta are selected. The electrons must be detected in the polar angle range $5° < \theta^e < 150°$ and have transverse momenta larger than 25, 20 and 15 GeV, respectively. To reduce the background from QED Compton processes, each electron in the central region ($\theta^e > 35°$) must be associated to a charged track. A Z candidate is reconstructed from the combination of the two electrons with an invariant mass closest to the nominal Z boson mass. The reconstructed mass of the Z candidate is required be compatible with the nominal Z boson mass within 7 GeV. After this selection no data event remains, while 0.72 ± 0.06 SM background events are expected. The selection efficiency for e^* with masses above 120 GeV is $\sim 60\%$.

In the search for $e^* \to eZ \to e\mu\mu$, events are selected with one electron with transverse momentum above 20 GeV and two muons with transverse momenta above 15 and 10 GeV, respectively. The electron and the muons must be detected in the polar angle ranges $5° < \theta^e < 150°$ and $10° < \theta^\mu < 160°$, respectively. A Z candidate

is reconstructed from the combination of the two muons and its reconstructed mass is required to be larger than 60 GeV. After this selection no data event remains, while 0.52 ± 0.05 SM background events are expected. The selection efficiency in this channel is $\sim 40\%$ for $M_{e^*} = 120$ GeV, decreasing to 15% for $M_{e^*} = 260$ GeV.

The signatures of the $e^* \to \nu W \to \nu e\nu$ and $e^* \to eZ \to e\nu\nu$ channels are similar and consist of one high P_T electron in events with large missing transverse momentum. Events with $P_T^{miss} > 25$ GeV and one electron with $P_T > 20$ GeV are selected. The electron is detected in the polar angle range $5° < \theta^e < 100°$ and is required to be isolated from jets by a minimum distance of $R > 1$. To reduce the background from radiative CC DIS processes, a track must be associated to the electron in the central region ($\theta^e > 35°$). Events from photoproduction are suppressed by requiring $V_{ap}/V_p < 0.1$. Remaining NC DIS events are removed by requiring that the longitudinal momentum balance of the event be $\sum_i(E_i - P_{z,i}) < 45$ GeV, where the sum runs over all visible particles. In order to remove background arising from SM W production, the hadron system is required to have a total transverse momentum $P_T^h < 20$ GeV and to exhibit a polar angle γ_h, as defined in [37], below 80°. In each event, only one neutrino candidate can be reconstructed, from the total missing transverse momentum, as explained at the beginning of Section 5. The invariant mass of the e^* candidate in the $e\nu\nu$ final state is therefore estimated from the four-vectors of the neutrino candidate and the electron candidate. To further remove background from W production, only events in which the reconstructed e^* mass is above 90 GeV are considered. After this selection four data events remain, while 4.5 ± 0.7 SM background events are expected. The selection efficiency for the $e^* \to \nu W \to \nu e\nu$ ($e^* \to eZ \to e\nu\nu$) signature is $\sim 60\%$ ($\sim 35\%$) for e^* with masses above 120 GeV.

5.5. *Systematic uncertainties*

The following experimental systematic uncertainties are considered:

- The uncertainty on the electromagnetic energy scale varies between 0.7% and 2% depending on the polar angle. The polar angle measurement uncertainty is 3 mrad for electromagnetic clusters.
- The scale uncertainty on the transverse momentum of high P_T muons amounts to 2.5%. The uncertainty on the reconstruction of the muon polar angle is 3 mrad.
- The hadronic energy scale is known within 2%. The uncertainty on the jet polar angle determination is 10 mrad.
- The uncertainty on the trigger efficiency is 3%.
- The luminosity measurement has an uncertainty of 3%.

The effect of the above systematic uncertainties on the SM expectation and the signal efficiency are determined by varying the experimental quantities by ± 1 standard deviation in the MC samples and propagating these variations through the whole analysis chain.

Additional model systematic uncertainties are attributed to the SM background MC generators described in Section 3. An error of 20% on the normalisation of NC DIS, CC DIS and photoproduction processes with at least two high P_T jets is considered to account for the uncertainty on higher order QCD corrections. The error on the elastic and quasi-elastic QED Compton cross sections is conservatively estimated to be 5%. The error on the inelastic QED Compton cross section is 10%. The errors attributed to lepton pair and W production are 3% and 15%, respectively. The total error on the SM background prediction is determined by adding the effects of all model and experimental systematic uncertainties in quadrature.

---

[23] For NC DIS events, this variable is proportional to the four-momentum transfer squared Q^2.

Table 1

Observed and predicted event yields for the studied e^* decay channels. The analysed data sample corresponds to an integrated luminosity of 475 pb^{-1}. The errors on the SM predictions include model and experimental systematic errors added in quadrature. Typical selection efficiencies for e^* masses ranging from 120 to 260 GeV are also indicated

| Channel	Data	SM	Signal efficiency [%]
$e^* \rightarrow e\gamma$ (ela.)	42	48 ± 4	60–70
$e^* \rightarrow e\gamma$ (inel.)	65	65 ± 8	60–70
$e^* \rightarrow \nu W \rightarrow \nu q\bar{q}$	129	133 ± 32	20–55
$e^* \rightarrow \nu W \rightarrow \nu e\nu$	4	4.5 ± 0.7	60
$e^* \rightarrow eZ \rightarrow e\nu\nu$			35
$e^* \rightarrow eZ \rightarrow eq\bar{q}$	286	277 ± 62	20–55
$e^* \rightarrow eZ \rightarrow eee$	0	0.72 ± 0.06	60
$e^* \rightarrow eZ \rightarrow e\mu\mu$	0	0.52 ± 0.05	40–15

The theoretical uncertainty on the e^* production cross section is dominated by the uncertainty on the scale at which the proton parton densities are evaluated. It is estimated by varying this scale from $\sqrt{Q^2}/2$ to $2\sqrt{Q^2}$. The resulting uncertainty depends on the e^* mass and is 10% at $M_{e^*} = 100$ GeV, increasing to 15% at $M_{e^*} = 300$ GeV.

6. Interpretation

The event yields observed in all decay channels are in agreement with the corresponding SM expectations and are summarised in Table 1. The SM predictions are dominated by QED Compton for the $e\gamma$ resonance search, by CC DIS in the $\nu q\bar{q}$ resonance search and by NC DIS processes for the $eq\bar{q}$ resonance search. The distributions of the invariant mass of the data events are in agreement with those of the expected SM background as shown in Fig. 1. Few or no data events are observed in channels corresponding to leptonic decays of the W or Z bosons, in agreement with the low SM expectations.

Since no evidence for the production of excited electrons is observed, upper limits on the e^* production cross section and on the model parameters are derived as a function of the mass of the excited electron. Limits are presented at the 95% confidence level (CL) and are obtained from the mass spectra using a modified frequentist approach which takes statistical and systematic uncertainties into account [39].

Upper limits on the product of the e^* production cross section and of the e^* decay branching ratio are shown in Fig. 2. The analysed decay channels of the W and Z gauge bosons are combined. Considering pure gauge interactions, the resulting limit on f/Λ after combination of all decay channels is displayed as a function of the e^* mass in Fig. 3, for the conventional assumption $f = +f'$. The total fraction of all possible e^* gauge decay channels covered in this analysis is $\sim 88\%$. The limit extends up to e^* masses of 290 GeV. Considering the assumption $f/\Lambda = 1/M_{e^*}$ excited electrons with masses up to 272 GeV are excluded. The relative contributions of the e^* decay channels to the combined limit are shown in Fig. 3(a). At low mass, the combined limit on f/Λ is dominated by the $e^* \rightarrow e\gamma$ channel, while the $e^* \rightarrow \nu W$ channel starts to contribute to the limit for masses above 200 GeV. These new results extend the previously published limits by H1 [2] and ZEUS [40] by more than a factor of two in f/Λ. Fig. 3(b) shows direct and indirect limits on e^* production obtained in e^+e^- collisions at LEP by the OPAL Collaboration [41] and DELPHI Collaboration [42], respectively. The result of the most recent search for e^* production within gauge mediated models obtained at the Tevatron by the CDF Collaboration is also indicated [43]. The limit from the present analysis extends at high mass beyond the kinematic reach of LEP searches and to lower f/Λ values than are reached by Tevatron searches.
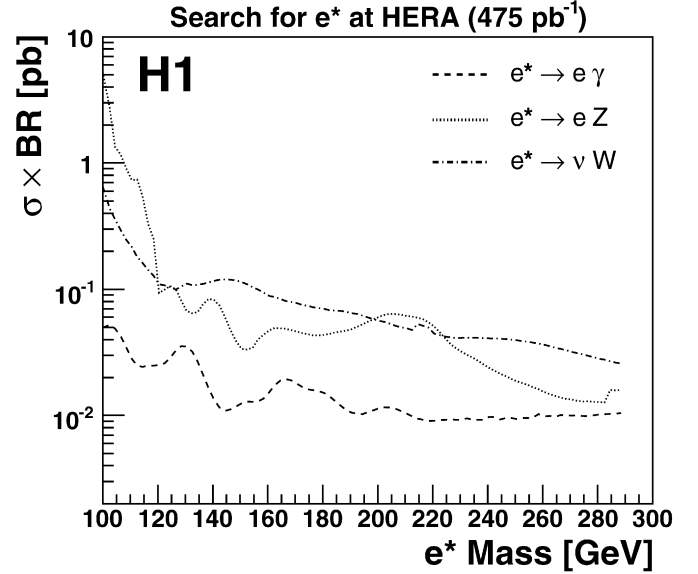
Fig. 2. Upper limits at 95% CL on the product of the e^* cross section and decay branching ratio, $\sigma \times$ BR, in the three e^* decay channels as a function of the excited electron mass. The decay channels of the W and Z gauge bosons are combined. The limits correspond to $e^\pm p$ collision data with an effective $\sqrt{s} = 318$ GeV and relative fractions of e^+p and e^-p data of 61% and 39%, respectively. Areas above the curves are excluded.

If e^* production is considered via gauge and contact interactions together, an upper limit on $1/\Lambda$ is also obtained, under the assumption $f = f' = 1$. Possible e^* decays by either gauge or contact interactions are taken into account and the efficiency of the analysis to e^* CI decays is conservatively assumed to be zero. The limit on $1/\Lambda$ as a function of the e^* mass is displayed in Fig. 4. For e^* masses below 250 GeV, the additional contribution of CI to e^* production changes the limit on Λ by a factor of 1.15 to 1.2. A limit on Λ as a function of the e^* mass is also obtained at the Tevatron by considering single e^* production via contact interactions only, followed by its gauge decay into an electron and a photon [44].

7. Conclusion

Using the full $e^\pm p$ data sample collected by the H1 experiment at HERA with an integrated luminosity of 475 pb^{-1} a search for the production of excited electrons is performed. The excited electron decay channels $e^* \rightarrow e\gamma$, $e^* \rightarrow eZ$ and $e^* \rightarrow \nu W$ with subsequent hadronic or leptonic decays of the W and Z bosons are considered and no indication of a signal is found. New limits on the production cross section of excited electrons are obtained. Within gauge mediated models, an upper limit on the coupling f/Λ as a function of the excited electron mass is established for the specific relation $f = +f'$ between the couplings. Assuming $f = +f'$ and $f/\Lambda = 1/M_{e^*}$ excited electrons with a mass lower than 272 GeV are excluded at 95% confidence level. For the first time in ep collisions, gauge and four-fermion contact interactions are also considered together for e^* production and decays. In this scenario and assuming the same Λ parameter in contact and gauge interactions as well as $f = +f' = 1$, $\eta_L = 1$ and $\eta_R = 0$, the limit on $1/\Lambda$ improves only slightly, demonstrating that the gauge interaction mechanism is dominant for excited electron processes at HERA. The results presented in this Letter extend previously excluded domain at HERA, LEP or Tevatron.
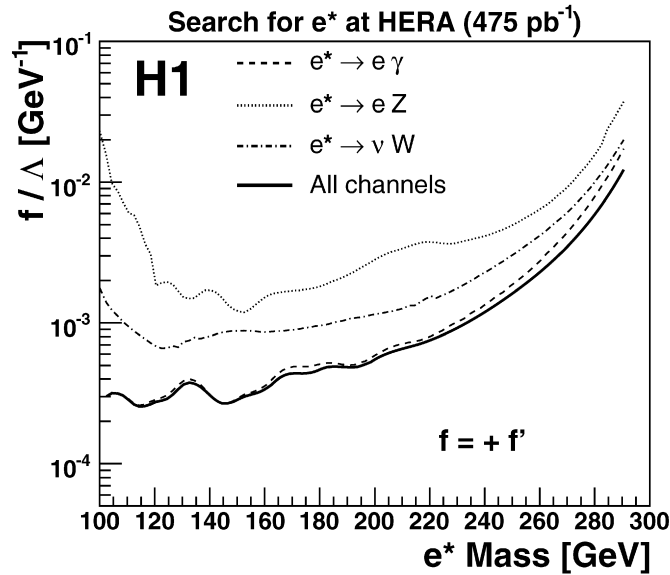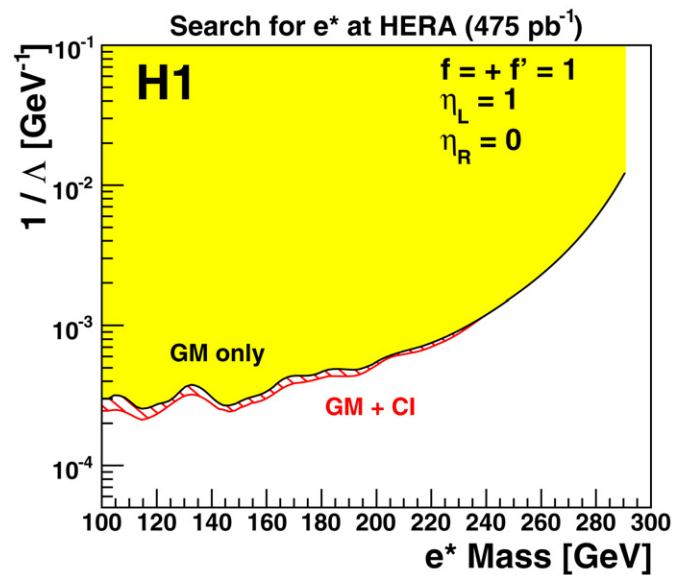
(a)
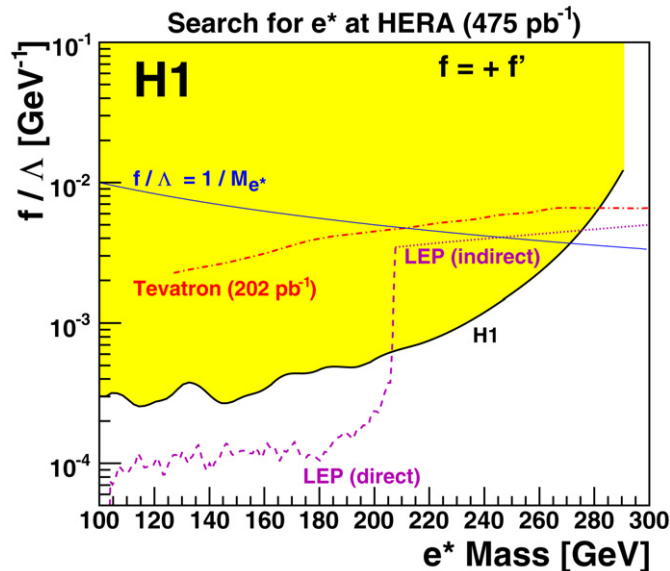
(b)

Fig. 3. Exclusion limits at 95% CL on the coupling f/Λ as a function of the mass of the excited electron considering gauge mediated interactions only, with the assumption $f = +f'$. The separate contributions of the different e^* decay channels are presented in (a). Values of the couplings above the curves are excluded. The excluded domain based on all H1 $e^{\pm}p$ data is represented in (b) by the shaded area. It is compared to the direct (dashed line) and indirect (dotted line) exclusion limits obtained at LEP by the OPAL Collaboration [41] and by the DELPHI Collaboration [42], respectively. The result from the Tevatron obtained by the CDF experiment [43] is also shown (dashed-dotted line). The curve $f/\Lambda = 1/M_{e^*}$ is indicated in (b).

engineers and technicians for their work in constructing and maintaining the H1 detector, our funding agencies for financial support, the DESY technical staff for continual assistance and the DESY directorate for the hospitality which they extend to the non-DESY members of the Collaboration. We also wish to thank M. Spira for many useful discussions and for providing the cross section calculation for excited electron production including contact interactions in ep collisions.

References

[1] H. Harari, Phys. Rep. 104 (1984) 159.

Fig. 4. Exclusion limits at 95% CL on the inverse of the compositeness scale $1/\Lambda$ as a function of the mass of the excited electron. The excluded domain obtained by considering e^* production via gauge mediated interactions only and under the assumption $f = +f' = 1$ is represented by the shaded area. The hatched area corresponds to the additional domain excluded if gauge mediated and contact interactions are considered together for e^* production. Areas above the curves are excluded.

[2] C. Adloff, et al., H1 Collaboration, Phys. Lett. B 548 (2002) 35, hep-ex/0207038.
[3] F.D. Aaron, et al., H1 Collaboration, Phys. Lett. B 663 (2008) 382, arXiv: 0802.1858 [hep-ex].
[4] K. Hagiwara, S. Komamiya, D. Zeppenfeld, Z. Phys. C 29 (1985) 115.
[5] U. Baur, M. Spira, P.M. Zerwas, Phys. Rev. D 42 (1990) 815.
[6] F. Boudjema, A. Djouadi, J.L. Kneur, Z. Phys. C 57 (1993) 425.
[7] S.J. Brodsky, S.D. Drell, Phys. Rev. D 22 (1980) 2236.
[8] F.M. Renard, Phys. Lett. B 116 (1982) 264.
[9] C. Adloff, et al., H1 Collaboration, Phys. Lett. B 568 (2003) 35, hep-ex/0305015.
[10] M. Spira, private communication.
[11] T. Köhler, Exotic processes at HERA: The event generator COMPOS, in: W. Buchmüller, G. Ingelman (Eds.), Proceedings of the Workshop "Physics at HERA", vol. 3, DESY, 1991, p. 1526.
[12] C. Berger, W. Wagner, Phys. Rep. 146 (1987) 1.
[13] J. Pumplin, et al., JHEP 0207 (2002) 012, hep-ph/0201195.
[14] T. Sjöstrand, et al., PYTHIA version 6.1, Comput. Phys. Commun. 135 (2001) 238, hep-ph/0010017.
[15] H. Jung, RAPGAP version 3.1, Comput. Phys. Commun. 86 (1995) 147.
[16] A. Kwiatkowski, H. Spiesberger, H.J. Möhring, Comput. Phys. Commun. 69 (1992) 155.
[17] G.A. Schuler, H. Spiesberger, DJANGOH version 1.4, Django: The interface for the event generators Heracles and Lepto, in: W. Buchmüller, G. Ingelman (Eds.), Proceedings of the Workshop "Physics at HERA", vol. 3, DESY, 1991, p. 1419.
[18] L. Lönnblad, Comput. Phys. Commun. 71 (1992) 15.
[19] C. Adloff, et al., H1 Collaboration, Eur. Phys. J. C 25 (2002) 13, hep-ex/0201006.
[20] A. Aktas, et al., H1 Collaboration, Phys. Lett. B 602 (2004) 14, hep-ex/0408044.
[21] C. Berger, P. Kandel, A new generator for wide angle bremsstrahlung, in: A.T. Doyle, G. Grindhammer, G. Ingelman, H. Jung (Eds.), Proceedings of the Workshop "Monte Carlo Generators for HERA Physics", DESY, 1998.
[22] U. Baur, J.A. Vermaseren, D. Zeppenfeld, Nucl. Phys. B 375 (1992) 3.
[23] T. Abe, GRAPE-Dilepton version 1.1, Comput. Phys. Commun. 136 (2001) 126, hep-ph/0012029.
[24] R. Brun, et al., GEANT3, CERN-DD/EE/84-1.
[25] I. Abt, et al., H1 Collaboration, Nucl. Instrum. Methods A 386 (1997) 310; I. Abt, et al., H1 Collaboration, Nucl. Instrum. Methods A 386 (1997) 348.
[26] B. Andrieu, et al., H1 Calorimeter Group Collaboration, Nucl. Instrum. Methods A 336 (1993) 460.
[27] B. Andrieu, et al., H1 Calorimeter Group Collaboration, Nucl. Instrum. Methods A 350 (1994) 57.
[28] B. Andrieu, et al., H1 Calorimeter Group Collaboration, Nucl. Instrum. Methods A 336 (1993) 499.
[29] R.D. Appuhn, et al., H1 SPACAL Group Collaboration, Nucl. Instrum. Methods A 386 (1997) 397.
[30] C. Adloff, et al., H1 Collaboration, Eur. Phys. J. C 30 (2003) 1, hep-ex/0304003.
[31] V. Andreev, et al., H1 Collaboration, Phys. Lett. B 561 (2003) 241, hep-ex/0301030.

[32] M. Peez, Recherche de déviations au Modèle Standard dans les processus de grande énergie transverse sur le collisionneur électron–proton HERA, PhD thesis, Université de Lyon (2003), DESY-THESIS-2003-023, available at http://www-h1.desy.de/psfiles/theses/.

[33] B. Portheault, Première mesure des sections efficaces de courant chargé et neutre avec le faisceau de positrons polarisé à HERA II et analyses QCD-électrofaibles, PhD thesis, Université Paris XI (2005), LAL-05-05, available at http://www-h1.desy.de/psfiles/theses/.

[34] S.D. Ellis, D.E. Soper, Phys. Rev. D 48 (1993) 3160, hep-ph/9305266.

[35] S. Catani, et al., Nucl. Phys. B 406 (1993) 187.

[36] T.N. Trinh, Recherche de leptons excités sur le collisionneur HERA avec le détecteur H1, PhD thesis, Université de la Méditerranée Aix-Marseille II (2008), available at http://www-h1.desy.de/psfiles/theses/.

[37] C. Adloff, et al., H1 Collaboration, Eur. Phys. J. C 13 (2000) 609, hep-ex/9908059.

[38] A. Blondel, F. Jacquet, in: U. Amaldi (Ed.), Proceedings of the Study of an *ep* Facility for Europe, vol. 79/48, DESY, 1979, p. 391.

[39] T. Junk, Nucl. Instrum. Methods A 434 (1999) 435, hep-ex/9902006.

[40] S. Chekanov, et al., ZEUS Collaboration, Phys. Lett. B 549 (2002) 32, hep-ex/0109018.

[41] G. Abbiendi, et al., OPAL Collaboration, Phys. Lett. B 544 (2002) 57, hep-ex/0206061.

[42] J. Abdallah, et al., DELPHI Collaboration, Eur. Phys. J. C 37 (2004) 405, hep-ex/0409058.

[43] D. Acosta, et al., CDF Collaboration, Phys. Rev. Lett. 94 (2005) 101802, hep-ex/0410013.

[44] V.M. Abazov, et al., D0 Collaboration, Phys. Rev. D 77 (2008) 091102(R), arXiv:0801.0877 [hep-ex].